Ultra Low Reynolds Number Airfoil Testing Facility

Michael Kerho*
Rolling Hills Research Corporation, 420 N. Nash St., El Segundo CA 90245
mike@rollinghillsresearch.com

ABSTRACT

This paper documents research being performed under a SBIR Phase II program funded by NASA Dryden Flight Research Center. The paper will discuss the design, set-up, and initial testing of a new ultra low Reynolds number water tunnel airfoil testing facility. The new water tunnel 2-D airfoil facility is designed to test airfoil sections at low Reynolds numbers ranging from 20,000 to 110,000. Force and moment results for the airfoil sections are obtained through surface static pressures and wake pressure measurements. These low Reynolds number, very low dynamic pressure measurements are complicated by the water test medium in the form of large pressure tube equalization time lags. Both the model and acquisition system have been designed to minimize the measurement system response times. In addition to the system design and implementation, initial pressure and wake measurements are presented.

NOMENCLATURE

c	Model Chord
C_p	Pressure coefficient, $(P_1-P_\infty)/q$
C_d	Drag coefficient per unit span, d/qL
C_l	Lift coefficient per unit span, l/qc
d	Tube diameter, drag per unit span
l	Lift per unit span
L	Tubing length, model characteristic length
P_1	Pressure at the orifice
P_o	Initial Pressure at time t_o at the transducer
P	Pressure at the transducer at any given time t
q	Dynamic pressure, $0.5\rho V_\infty^2$
Re	Reynolds number, $\rho V_\infty c/\mu$
t	Time
u	Streamwise velocity
V	Total measuring system volume
V_∞	Free-stream velocity

Symbols:

α	Model angle-of-attack
ρ	Density
μ	Viscosity

*Chief Aerodynamicist, AIAA Associate Fellow

INTRODUCTION

The development of micro unmanned air vehicles (μ-UAVs) and Mars aircraft has received considerable attention in recent years. Unlike conventional aircraft and UAVs, μ-UAVs and Mars aircraft suffer from operation in an extremely low Reynolds number flight regime. Generally, a low Reynolds number is considered to be between 150,000 and 500,000. Both μ-UAVs and Mars aircraft, however, can have operational Reynolds number regimes from 20,000 to 120,000. At these extremely low Reynolds numbers, the aerodynamic flow features are dominated by laminar separation and separation bubble effects, which are the primary source of poor performance in both drag and maximum lift for this class of vehicles. The current paper discusses the design and initial testing of a new ultra low Reynolds number airfoil testing facility.

The new ultra low Reynolds number test facility is being set-up in the Rolling Hills Research Corporation (RHRC) Model 2436 water tunnel and is designed to test sections in the range from Re_c=20,000 to 110,000. For this low Reynolds number regime, the use of a water tunnel, as compared to a wind tunnel, presents several distinct advantages and challenges. For this very low Reynolds number regime, the use of a water tunnel allows a much larger model to be tested at a higher dynamic pressure. For a Reynolds number of approximately 85,000, for example, a model chord of 12 inches can be used in the water tunnel with a free stream velocity of 1 ft/s, yielding a dynamic pressure of 0.95psf. For the same chord length in a wind tunnel, the dynamic pressure would drop to 0.2psf. In order to achieve the same dynamic pressure, the wind tunnel model chord would have to be reduced by almost half. The larger model scale afforded by the water tunnel allows for easier model construction and installation of measurement instrumentation such as surface static pressure ports. Due to the very low dynamic pressure, cavitation over the airfoil in the water tunnel is not a concern. Finally, the water tunnel affords excellent flow visualization capability not obtainable in a wind tunnel through the use of multiple colored dyes.

The primary force and moment measuring system for the 2-D airfoil testing facility is pressure based. Lift and pitching moment are calculated by integrating measured surface static pressures, with drag being obtained from a traversing pitot-static probe in the wake. Although the dynamic pressure in the water tunnel is higher for a given chord length as compared to the wind tunnel, it is still small and poses measurement challenges. For a water tunnel dynamic pressure of 0.95psf, the flow induced surface pressures will be on the order of 0.5 to 1 inch H_2O, with differential dynamic pressures in the wake at 0.15 to 0.2 inches H_2O. While the measurement of pressures in this low range is not in itself inherently difficult, the problem arises with large columns of water present in the lines running from the model to the transducer over-ranging the very sensitive transducers.

Accurate measurement of surface pressures in a low speed water tunnel have been successfully acquired by Erm[1] for the flow over a 70° delta wing at high angle-of-attack. The experiment acquired model upper surface static pressures in the water tunnel while concurrently visualizing the vortical flowfield using sodium fluoresein dye. The nominal free-stream velocity used in these experiments was approximately 4 in/s. Based on a wing centerline chord of 11.8 inches, the Reynolds number was 3.0×10^4. Results from these experiments compared well with similar wind tunnel measurements.[1]

Another difficulty with pressure measurement in water has to do with increased tube lag response times as compared to similar measurements made in air. Both the model and acquisition system need to incorporate design features which attempt to minimize tube lags. Any facility designed to accurately test airfoil sections at these very low Reynolds numbers will face significant difficulties. It is believed, however, that the water tunnel will prove to be an excellent tool for this challenging regime. This paper will discuss design, difficulties, and implementation of a pressure measurement based force and moment acquisition system in a water tunnel environment, including aspects of model design. Additionally, some initial pressure and wake measurements made in the facility will be presented.

MODEL 2436 WATER TUNNEL AND GENERAL EXPERIMENTAL SET-UP

The Model 2436 water tunnel is a closed circuit continuous flow horizontal configuration with a free surface. The horizontal free surface configuration allows model and instrumentation installation and access to be performed without draining the tunnel. The test section has a width of 24 inches, height of 36 inches, and length of

74 inches. The test section flow velocity is variable from 0 to 1.2 ft/s. The tunnel is equipped with honeycomb and screens along with a contraction ratio of 6:1 to provide high flow quality and low free-stream turbulence levels. A schematic and picture of the Model 2436 water tunnel is shown in Figure 1. The RHRC Model 2436 water tunnel has been used extensively for performing quantitative 3-D dynamic experiments using a submersible 5-component strain gage balance. These dynamic experiments include forced oscillation motions, ramp and hold maneuvers, rotary balance tests, Schroeder sweeps, and Tobak-Schiff motions. For the current program, the Model 2436 was modified for the testing of 2-D airfoil sections. The modifications required to the tunnel were relatively minor and included the addition of a model sidewall mounting system with a remotely controlled angle-of-attack servo-motor system, and a pressure measurement acquisition system. The pressure system is used measure surface pressures on the airfoil model. Surface pressures are integrated to calculate the airfoil lift and pitching moment. A pitot-static probe mounted on a traversing system in the wake is used to calculate the airfoil drag. The pressure measurement system will be discussed in length in a separate section.

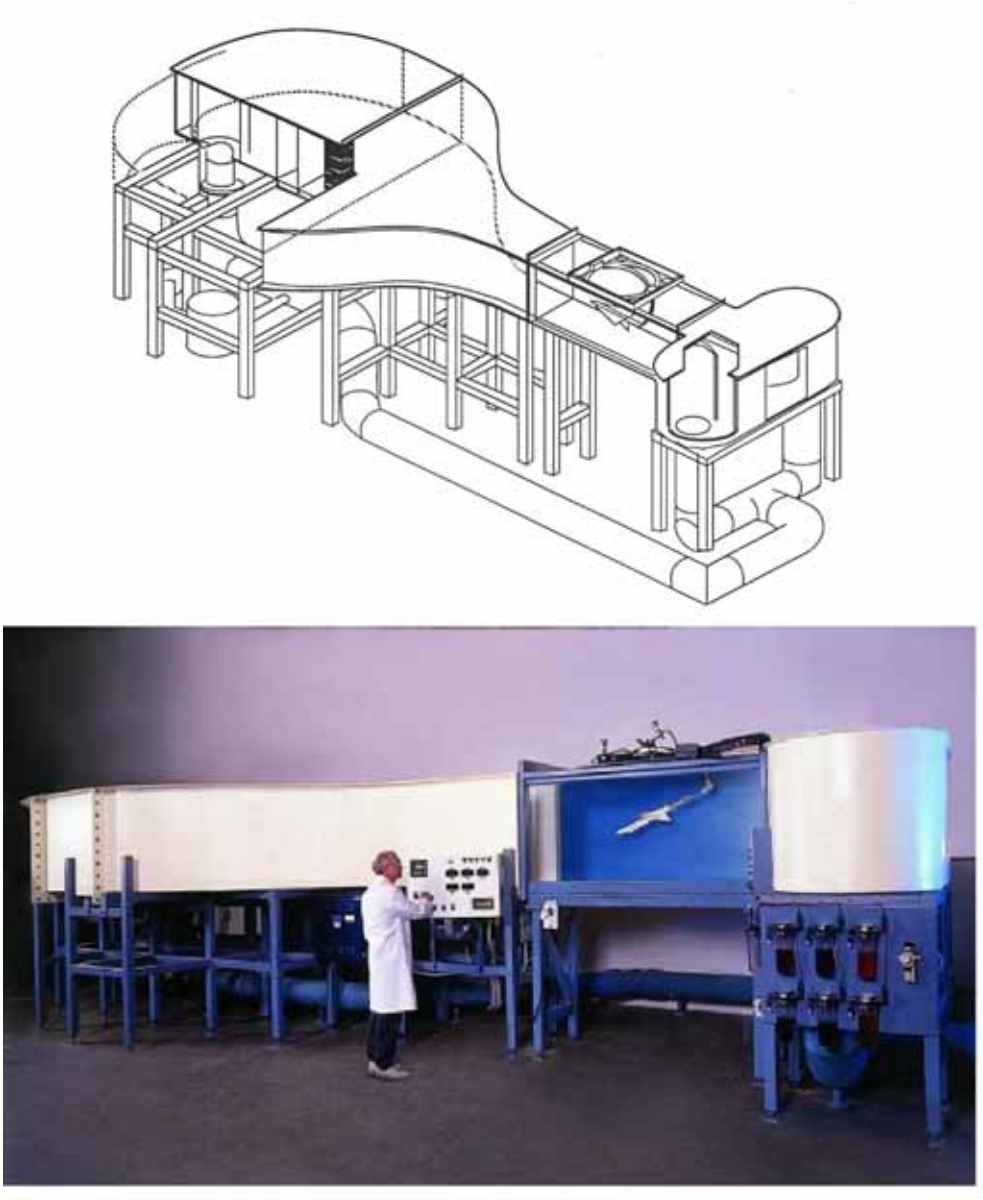

Figure 1: Schematic and photograph showing the Rolling Hills Research Model 2436 water tunnel.

The 2-D airfoil model is mounted horizontally, spanning the tunnel width. The model is inverted with the upper surface facing the tunnel floor. This mounting scheme allows excellent visualization of the model upper surface. The sidewall mounting system includes the addition of two sidewall insert plates that extend from upstream of the model to well downstream. The sidewall inserts allow for a modular mounting system in the tunnel and also allow for the model to be run upright and inverted. A pitot-static probe mounted upstream of the model on one of the false sidewalls provides test section static and dynamic pressure. A second pitot-static probe located one chord length downstream of the model is used to generate wake deficit profiles for determination of sectional drag. A schematic of the test section set-up and modifications is shown in Figure 2. From Figure 2, the model is shown with a 13 inch chord spanning the width of the tunnel. Model instrumentation (pressure tubing) is routed through a channel in the rear sidewall insert.

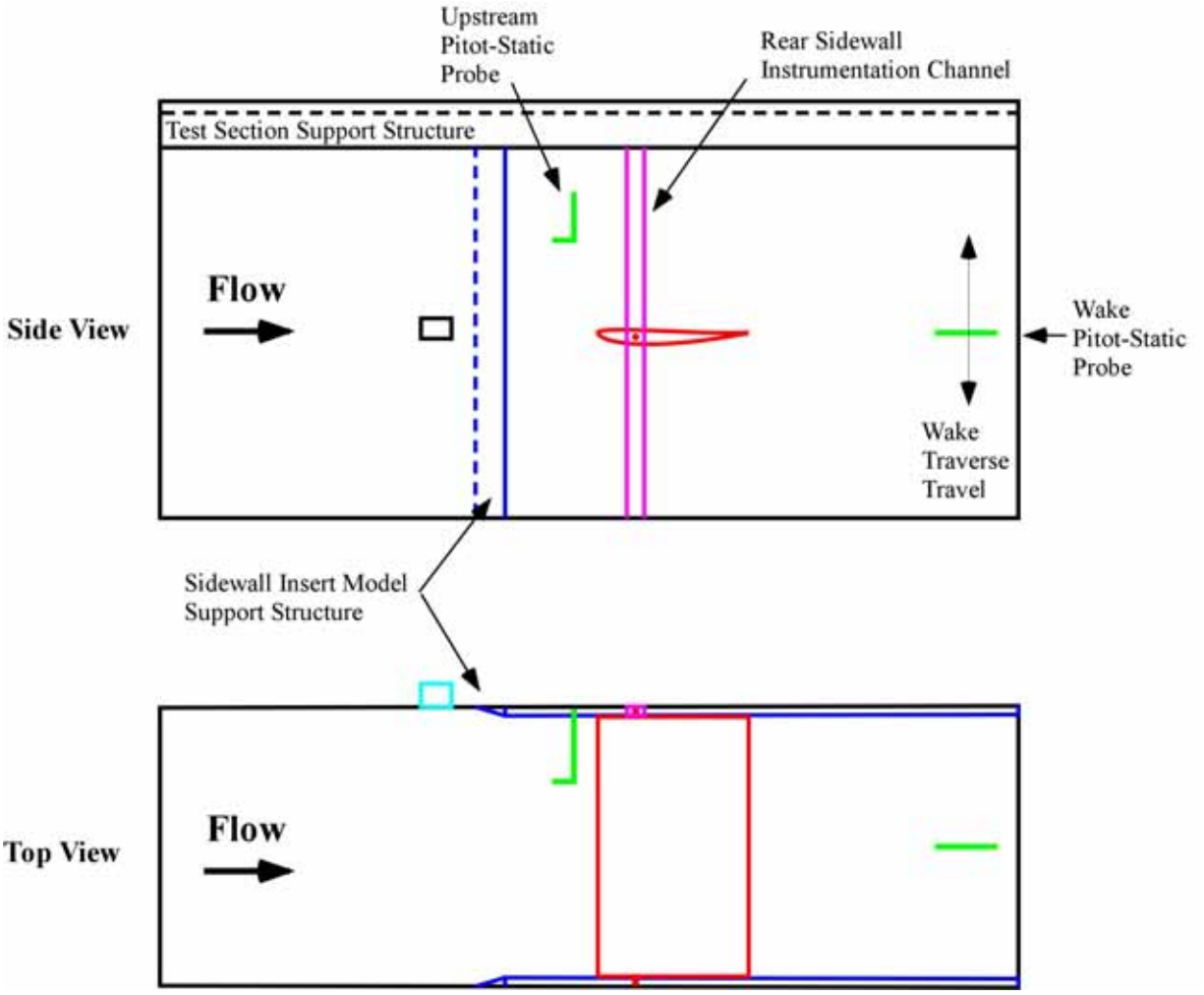

Figure 2: Model 2436 tunnel test section schematic showing sidewall inserts and model supporting structure.

INSTRUMENTATION

The measurement of static and dynamic pressures in a low-speed water tunnel is not a trivial task due to the very low tunnel q. As previously stated, for a free-stream velocity of 12 in/s, the tunnel dynamic pressure is on the order of 0.95 psf, which will produce flow induced pressures on the order of 0.5 to 1 inch H_2O, with differential dynamic pressures in the wake at 0.15 to 0.2 inches H_2O. Again, while the measurement of pressures in this low range is not in itself inherently difficult, the problem arises with large columns of water present in the lines running from the model to the transducer over-ranging the sensitive transducers. Also, care must be taken to remove all air

bubbles from the lines. For the very low flow induced pressures being read, small air bubbles in the lines can be the source of significant error.

The instrumentation set-up chosen for the current project uses two individual transducers for model surface static pressures and wake deficit pressures. The single model transducer is multiplexed to the model pressure lines using a set of solenoid valves and manifolds. The transducers chosen are two LPM 9481 Low Differential Pressure Transmitters, manufactured by Druck Inc. The two transducers have different ranges. The model transducer has a range of ±1 inch H_2O, with a maximum over-pressure of 55 inches H_2O, with the second wake transducer range being ±0.2 inches H_2O with a maximum over pressure of 20 inches H_2O. Both transducers have an accuracy of ±0.1% full scale. The high sensitivity of these transducers coupled with their high over-pressure values makes the measurement of pressures in the water tunnel practical.

As opposed to using a strain gage based force/moment measurement system for the determination of sectional lift and moment, the pressure-based system provides the advantage of producing detailed pressure mappings of the airfoil, allowing easier determination of separation bubble locations and characteristics. The value and insight provided by these pressure distributions, however, are tempered by the increased complexity and cost of the model, and added acquisition time required to multiplex the individual ports through a single transducer or multiple transducers.

The individual pressure lines from the model are multiplexed to the transducer through a set of solenoid valves and manifolds. 5 manifolds with 12 valves per manifold for a total of 56 individual valves are used. The solenoid valves used are ASCO scientific 2 way miniature solenoid valves (AM4112). These are 12 volt normally closed solenoid valves rated for water with a response time of 5 ms. The multiplexing of the valves is accomplished through a computer digital I/O interface incorporated into the overall acquisition and reduction system which was programmed using LabVIEW. The overall uncertainty of the pressure based force and moment measurement system has been estimated to be 1.5% for C_l, and 1.7% for C_d.

Pressure Measurement Tubing Considerations

The entire 2-D model data acquisition system has been designed around obtaining the highest quality pressure measurements in a timely manner. Initial experience with the pressure measurement system indicated that the time lag of a water based pressure measurement system can be extreme when compared to a traditionally designed wind tunnel based system using typical tube diameters. For normal pressure tube sizes of 0.040” to 0.060” and tube lengths (3-4 ft), pressure equalization times can increase from tenths of a second in air, to hundreds of seconds in water.

There are two types of lag in a capillary-based pressure measurement system, an acoustic and viscosity based lag. The acoustic lag is based on the fact that pressure disturbances travel at the speed of sound. As a result, a change in pressure at the orifice takes a finite amount of time to travel the distance through the connecting tube to the transducer. For most systems, the acoustic lag is small. The effect of the viscosity based lag, however, is to retard the equalization of the pressure in the tube and increase the amount of time required for the pressure to equalize in the tube/capillary system and at the transducer. While the speed of sound in water is 4 times that of air, the viscosity of water is two orders of magnitude greater than that of air. Sinclair and Robbins[2] derived an analytical theory to estimate the time lag in a capillary-based pressure measurement system. The theory takes system volume, tubing length and diameter, fluid viscosity, and pressure differential into account to estimate the time required for the pressure at the transducer to reach a prescribed percentage of the pressure at the measurement location. The equation Sinclair and Robbins[2] arrived at for the time lag as a function of the above parameters is given in Equation 1.

$$t = \frac{128\mu\ L}{\pi d^4}\left[\frac{V}{P_1}\ln\frac{(P_o - P_1)(P + P_1)}{(P - P_1)(P_o + P_1)}\right]$$

Equation 1

From Equation 1, the time lag is directly proportional to the tube length, fluid viscosity, and system volume, and inversely proportional to the pressure at the orifice. As the absolute pressure at the orifice decreases,

the time lag increases. The time lag is also inversely proportional to the diameter of the tubing to the 4th power. As a result, small increases in tube diameter can lead to large reductions in time lag. The effect of pressure differential and orifice pressure, tube diameter, and tube length on the response time for some typical tube lengths and diameters representative of the current test set-up are shown in Figure 3a-c. For Figure 3a-c, the assumed fluid is water at 60°F, and the response time shown is that time for the pressure in the transducer to reach 99% of the value of the pressure at the orifice. Figure 3a shows the effect of pressure differential and absolute orifice pressure on the tube lag response time for a 0.5 inH_2O pressure differential for three different orifice pressures of 0.25, 0.5, and 0.75 inH_2O at the orifice. The results presented in Figure 3a assume a tube length and diameter of 3 ft and 3/16 inches, respectively. From Figure 3a, both the time response to the differential and the effect of the absolute pressure on the time response are nonlinear, with the effect of the absolute pressure being quite large. Also apparent is the fact that the time required for the pressure in the tube to equalize is proportional to the size of the differential. It is interesting to note that, for the test cases shown, the majority of the time required for equalization occurs during the last 20% of the pressure differential. Since the absolute pressure at the orifice is governed by the model geometry and test conditions, minimization of the response time can be accomplished by keeping the pressure differential small, i.e. making steps in angle-of-attack relatively small, which is generally done for accurate mapping of the polar.

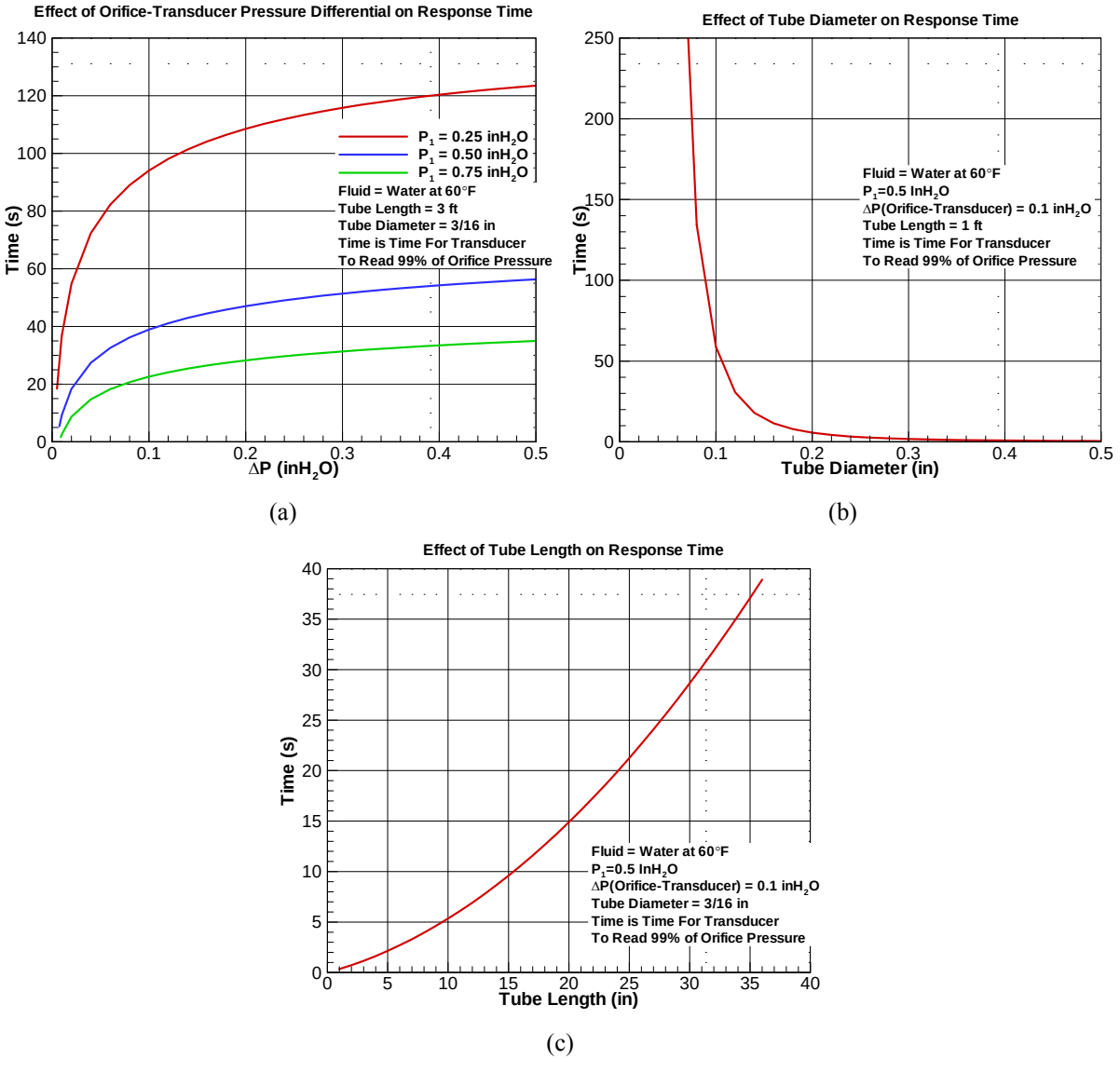

Figure 3: Effect of pressure differential, tube diameter, and tube length on pressure measurement response time.

Figure 3b shows the effect of tube diameter on the equalization response time. The results presented in Figure 3b assume an orifice pressure of 0.5 inH_2O, a pressure differential of 0.1 inH_2O, and a tube length of 1ft. From Figure 3b, the effect of increasing the tube diameter is dramatic. Increasing the tube diameter from 0.06 inches to 0.18 inches decreases the settling time by 393 seconds. Also apparent in Figure 3b, is the fact that above a certain diameter, little additional benefit is obtained. For the current study, tube diameters have been maximized to minimize the transducer response time. For the static pressure taps on the model, the tap orifices are 0.050 inches in diameter. The tap diameter increases inside the model (internal routing) to 0.090 inches. Finally, once outside the model and in the instrumentation channel, the tube diameter further increasing to 0.1875 inches from the model to the solenoid valves. From the valves to the transducer, the tube diameter increases yet again to 0.375 inches. Preliminary testing of this tubing diameter set-up yields an equalization response time of approximately 10 seconds for a pressure differential of 0.1 inH_2O. For the wake traverse, the tube diameter is also 0.090 inches from the pitot-static probe until leaving the probe support, where it increases to 0.1875 inches to the transducer, yielding response times of approximately 10 seconds also. These tube sizes were the largest possible tube diameters allowable given the space constraints of the model and hardware.

Figure 3c shows the effect of tube length on the equalization response time. The results presented in Figure 3c again assume an orifice pressure of 0.5 inH_2O, a pressure differential of 0.1 inH_2O, and a tube diameter of 3/16 inches. Again, much like the effect of diameter and pressure differential, the effect of tube length on the equalization response time is nonlinear, with minimization being accomplished by simply limiting tube length. The results from Figure 3a-c indicate that in order to minimize the response time of the transducers, the tube diameter should be maximized while minimizing tube length and the applied pressure differential. The design of the model and acquisition hardware have attempted to incorporate these conclusions in order to minimize the tube equalization lag and thus minimize the time required to acquire a full angle-of-attack polar.

INITIAL PRESSURE AND WAKE MEASURMENTS

Before testing of the complete 2-D airfoil acquisition system, the pressure and wake measurement systems were validated in separate experiments. The pressure measurement system was used to obtain trailing-edge pressures on a 2-D airfoil like model used in a flow control experiment mounted in the Model 2436 airfoil testing facility. Wake measurements were made on a simple circular cylinder model and compared to accepted values.

Pressure System Checkout

The flow control experiment was designed to investigate the use of a pulsed tangential jet located in a massively separated region to virtually shape the amount of separation present from fully separated to fully attached. The test set-up mimicked the testing of a simple 2-D airfoil and provided an excellent checkout of the pressure measurement system. The model was designed to separate on the upper surface at approximately the 79% chord location. A pulsed tangential jet located at the 82% chord location would then be used to virtually shape the section by controlling the amount of separation. The 2-D test geometry had a chord length of 29 inches, producing a nominal Reynolds number of 0.2×10^6 at a tunnel speed of 11.5 in/s. The model was instrumented with approximately 27 surface static pressure ports covering the upper and lower surface trailing-edge region of the model. A schematic of the flow control model showing the general layout, jet location, and static tap locations is shown in Figure 4. Both flow visualization and pressure measurements were taken on the trailing-edge region to document the baseline separation and the effect of the pulsed jet flow control. A photograph showing the flow control model installed in the low Reynolds number testing facility is shown in Figure 5.

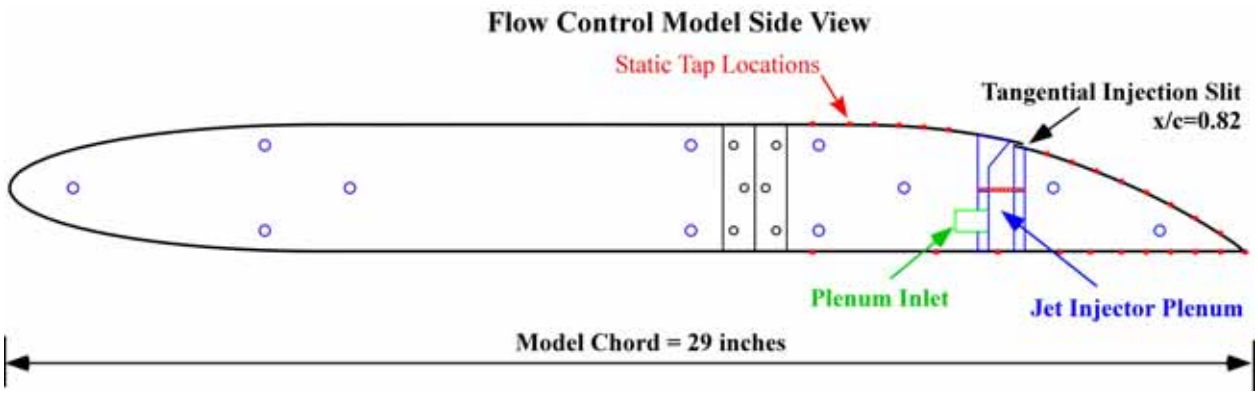

Figure 4: Schematic of 2-D flow control model showing surface tap locations.

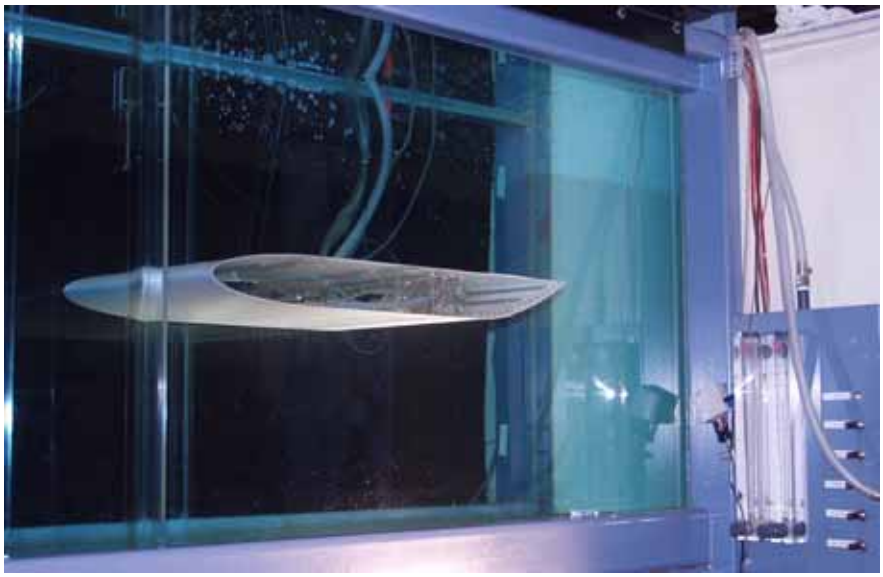

Figure 5: Photograph showing the 2-D flow control model mounted in the RHRC 2436 water tunnel.

Flow visualization results for the baseline, unforced, separated pressure recovery region and an attached pulsed blowing case are shown in Figure 6. From Figure 6, the baseline case with no blowing is shown to exhibit a laminar separation at x/c≈0.79 with no reattachment by the trailing-edge. The surface pressures for the baseline case with no blowing are well behaved with the upper surface pressures almost flat, showing little to no recovery, indicative of massive separation for the baseline unforced geometry. Flow visualization results for the pulsed jet case, however, appear to indicate fully attached flowfield. The pressure results for the pulsed blowing case show that the pulsed jet has significantly increased the circulation of the section, creating a low-pressure region upstream of the recovery. The lower surface pressures have also been affected. From the pulsed jet pressures, the flow appears to be fully attached, eliminating the separation, with both the upper surface and lower surface pressures converging to a single value at the trailing-edge. This trailing-edge pressure is also significantly more positive than the baseline geometry. As with the no blowing baseline case, the pulsed flow visualization and surface pressures compliment each other, indicating similar flowfield characteristics.

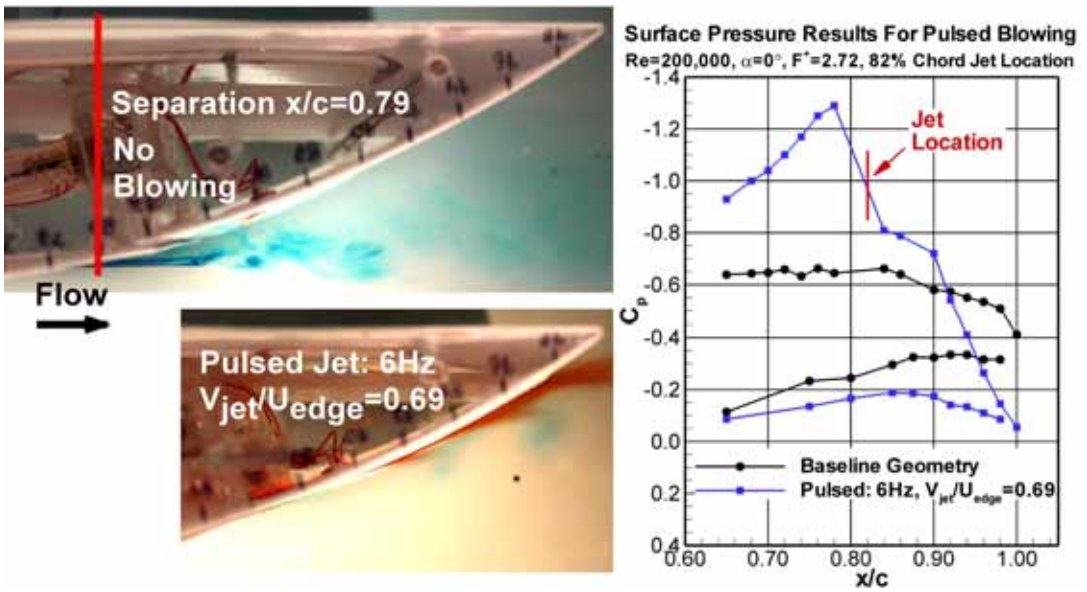

Figure 6: Flow visualization and surface pressures for the trailing-edge of a 2-D airfoil flow control model showing separated and attached flow.

Surface pressures for the flow control model with various levels of blowing, both continuous and pulsed are shown in Figure 7. From Figure 7, by adjusting the jet velocity and pulsing frequency, controlled changes in the circulation and pressure recovery can dictated. The sensitivity of the pressure measurement system allowed these changes to be accurately resolved and documented. The results from the initial checkout of the pressure measurement system show that design and implementation of the multiplexed scanning system should provide both the accuracy and sensitivity required by a low Reynolds number testing facility.

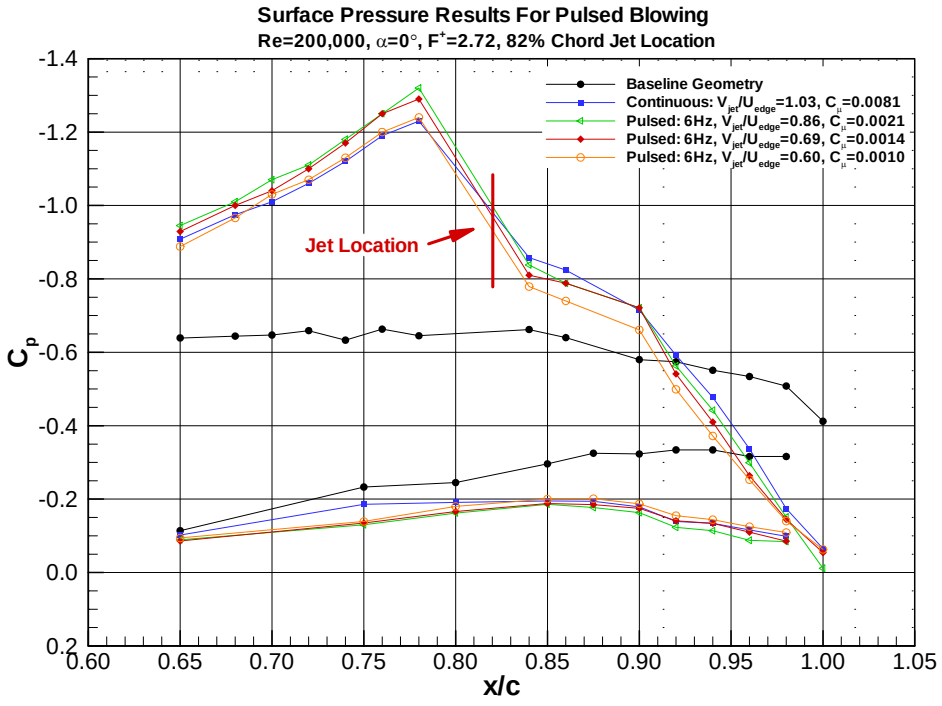

Figure 7: Surface pressures for the trailing-edge of a 2-D airfoil flow control model showing the effect of various pulsed jet velocities.

Wake System Checkout

As a preliminary checkout of the wake system, drag measurements on a simple circular cylinder were obtained. The circular cylinder was 1.05 inches in diameter and spanned the tunnel width. For this cylinder diameter, the range of available Reynolds numbers, based on diameter, is from approximately 2000 to 7000. Across this range, the drag is relatively constant. A photograph showing the cylinder model installed in the water tunnel is shown in Figure 8.

Figure 8: Photograph showing the circular cylinder model mounted in the RHRC 2436 water tunnel.

Wake profiles were taken at 24 diameters downstream. A plot of the cylinder wake velocity profile at Re_D=5021 is shown in Figure 9. From Figure 9, the wake velocity profile is well behaved. The drag of the cylinder was calculated from the wake velocities using the momentum deficit method[3] and assuming the survey plane was sufficiently downstream to allow recovery of the static pressure to its undisturbed value. The calculated drag of the wake velocity profile shown in Figure 9 was C_d=0.988. This value is 3.1% below that presented in Schlichting[3] for a circular cylinder at the Reynolds number tested (C_d=1.02). This slight under prediction of the drag is consistent with using the wake-survey method for determination of the drag for a bluff body with a highly turbulent wake as investigated by Lu and Bragg[4]. As discussed by Lu and Bragg[4], for highly turbulent wakes, total pressure probes aligned with the mean flow direction can read increased total pressure due to the effects of the turbulent velocity components in the axial and cross-stream plane, which can cause errors in calculating the mean velocity. The 3.1% lower drag value for the circular cylinder obtained in the current study is similar to that observed by Lu and Bragg[4]. Although limited, the cylinder drag results provide some confidence in the wake measurement and reduction system.

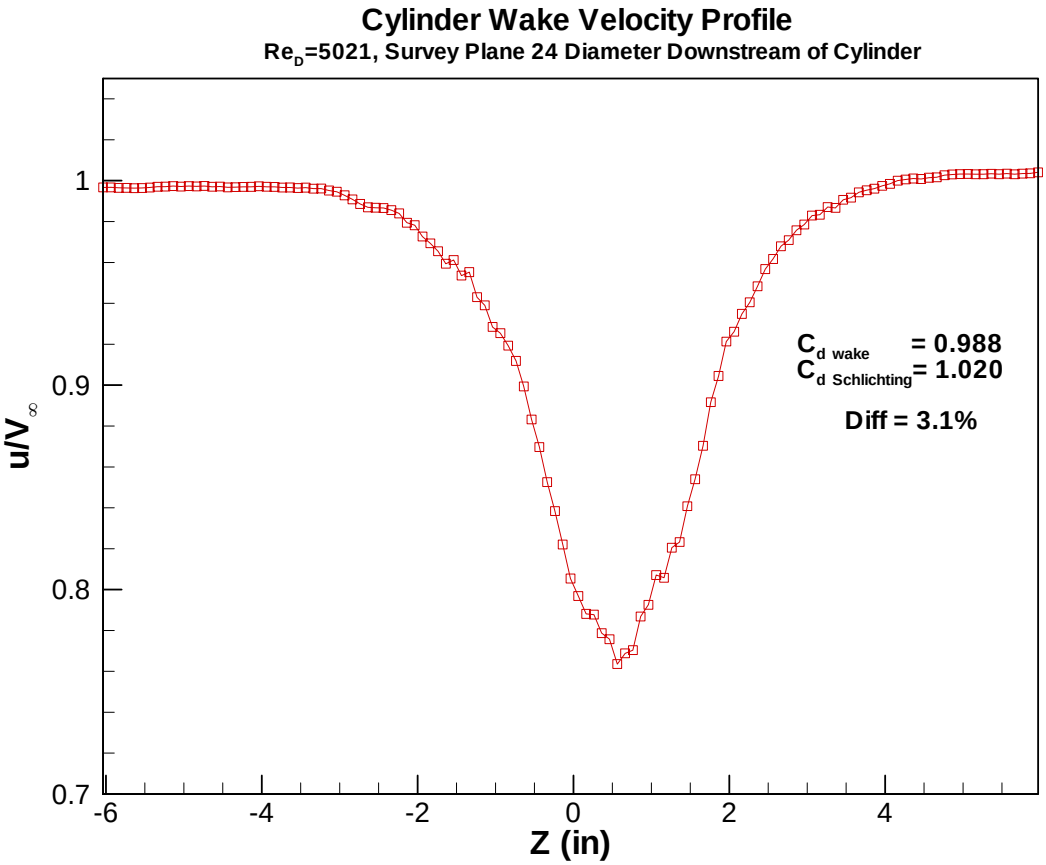

Figure 9: Cylinder wake velocity profile at 24 diameters downstream.

CURRENT STATUS

After the initial pressure and wake measurements were accomplished, a 2-D airfoil qualification test is being performed. The airfoil section chosen for the qualification testing of the new 2-D testing facility is the Selig/Donovan SD7037 section. The SD7037 section was chosen as it represents one of the best airfoil sections designed to operate at these ultra low Reynolds numbers. The SD7037 section is a state-of-the-art low Reynolds number section designed for competition R/C soaring. Wind tunnel results for the section at comparable Reynolds numbers are available for comparison and qualification.

The SD7037 water model to be constructed for the new ultra low Reynolds number test facility is to have a chord length of 13 inches and a span of 22 inches. The model was designed with a removable plate on the lower surface. The removable plate will facilitate access to the internals of the model, allowing the maximum tube diameter to be used as close the surface port as possible. A simple side view schematic of the model is shown in Figure 10. The model is currently designed for 32 upper surface and 24 lower surface static pressure taps (56 taps total). The upper and lower surface pressure tap lines are swept at an angle of 15° to the free-stream to help prevent premature transition of the upstream taps from affecting the state of the boundary-layer of the downstream taps.

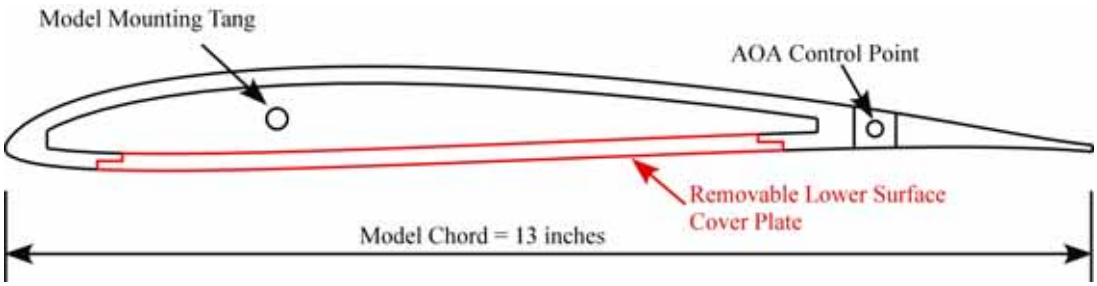

Figure 10: Side view of SD7037 water tunnel model schematic.

Due to the test fluid being water, construction of the model is limited to materials which will not corrode. This significant drawback is somewhat mitigated by the very low dynamic pressure and loads experienced by the model. Options for materials include stainless steel, hard anodized aluminum, or plastics. While being extremely corrosion resistant, stainless steel is undesirable from an economic standpoint due to its significant material cost and difficulty machining. While the material cost is less and the material more easily machineable, anodized aluminum is still relatively expensive for the size of the model required, and it has been our experience that anodized parts do not hold up well over time when they are submerged for significant amounts of time. While plastics provide excellent corrosion resistance and low material cost, they have poor machinablity when trying to hold high contour tolerances (±0.003-0.005 inches). With advances in materials and manufacturing, stereolithography (SLA) and selective laser sintering (SLS) methods are being investigated. Both SLA and SLS are rapid prototyping manufacturing technologies. SLA prototypes are constructed from a liquid polymer that is selectively cured using an ultraviolet laser. SLS prototypes are constructed from a powdered material that is selectively heated and fused by a powerful CO_2 laser. Depending upon the material used, SLA and SLS tolerances are quoted in the ±0.002-0.004 inch range, with a possible bias of +0.002-0.003 inches/inch. For the size of the model required, these quoted tolerances provide the required levels of accuracy. New materials such as the Watershed (SLA) and DuraForm GF (SLS) provide excellent waterproofing characteristics. SLA and SLS models are relatively cheap compared to traditionally machined stainless steel and aluminum models, and turnaround is extremely fast. A significant advantage of the SLA and SLS technologies is that they allow pressure taps and internal routing to be built directly into the model. Additionally, since cost is determined by the amount of solid material in the model, the quantity and internal routing of the pressure taps comes at no additional cost. Test articles of the SD7037 model manufactured using the SLA and SLS processes are currently being made to determine the most suitable from an accuracy, cost, and waterproofing standpoint.

CONCLUSIONS

A new ultra low Reynolds number water tunnel airfoil testing facility is being set-up and validated. The new facility is set-up to test 2-D airfoil sections at low Reynolds numbers ranging from 20,000 to 110,000. The new ultra low Reynolds number test facility is being set-up in the Rolling Hills Research Corporation (RHRC) Model 2436 water tunnel. For this low Reynolds number regime, the use of a water tunnel, as compared to a wind tunnel, allows a larger model to be tested at a higher dynamic pressure. The larger model scale afforded by the water tunnel allows for easier model construction and installation of measurement instrumentation such as surface static pressure ports. Due to the very low dynamic pressure, cavitation over the airfoil in the water tunnel is not a concern. Finally, the water tunnel affords excellent flow visualization capability not obtainable in a wind tunnel through the use of multiple colored dyes.

The primary force and moment measuring system for the 2-D airfoil testing facility is pressure based. Lift and pitching moment are calculated by integrating measured surface static pressures, with drag being obtained from a traversing pitot-static probe in the wake. Initial check-out of the surface static pressure measurement and wake measurement systems have been performed and indicate that the measurement systems provide both the accuracy and sensitivity required by a low Reynolds number testing facility.

Initial experience with the pressure measurement system indicated that the time lag of a water based pressure measurement system can be extreme when compared to a traditionally designed wind tunnel based system using typical tube diameters. As a result, a tube lag study was performed to maximize measurement accuracy while

minimizing measurement time. This study included both analytical and experimental investigations. For a capillary-based pressure measurement system where the working fluid is water, results from the tube lag study indicate that in order to minimize tube lag, the tube diameter should be maximized while minimizing tube length and the applied pressure differential between the orifice and transducer.

To date, all acquisition and reduction systems have been tested and verified. Manufacture of a 2-D airfoil model for full qualification testing of the facility is underway. An area requiring further investigation includes a proper wall correction methodology to account for the fact that the water tunnel facility has one solid and one free-surface.

ACKNOWLEDGEMENTS

This work was supported by NASA Dryden Research Center under a Phase II SBIR award under contract number NND06AA01C. The author would like to thank the technical monitor Mrs. Jennifer Hansen from NASA Dryden for her support and contributions throughout this program.

REFERENCES

[1] Erm, L., "An Investigation into the Feasibility of Measuring Flow-Induced Pressures on the Surface of a Model in the AMRL Water Tunnel," DSTO-TN-0323, Nov. 2000.

[2] Sinclair, A. R. and Robbins, A. W., "A Method of the Determination of the Time Lag in Pressure Measuring Systems Incorporating Capillaries," NACA TN 2793, Sept. 1952.

[3] Schlichting, H., *Boundary-Layer Theory*, 7th Ed., McGraw-Hill Publishing, New York, 1987, pp. 758-764.

[4] Lu, B. and Bragg, M., "Experimental Investigation of the Wake-Survey Method for a Bluff Body With a Highly Turbulent Wake, AIAA 2002-3060, paper presented at the 20th Applied Aerodynamics Conference, St. Louis, Missouri, June 2002.